J|A|C|S COMMUNICATIONS

Published on Web 11/11/2009

Buckyballs Meet Viral Nanoparticles: Candidates for Biomedicine

Nicole F. Steinmetz,*,† Vu Hong,‡ Erik D. Spoerke,§ Ping Lu,|| Kurt Breitenkamp,‡ M. G. Finn,*,‡ and Marianne Manchester*,†

Department of Cell Biology, Center for Integrative Molecular Biosciences, Department of Chemistry, and The Skaggs Institute for Chemical Biology, The Scripps Research Institute, 10550 North Torrey Pines Road, La Jolla, California 92037, and Department of Electronic and Nanostructured Materials and Department of Materials Characterization, Sandia National Laboratory, Albuquerque, New Mexico 87185

Received March 23, 2009; E-mail: nicoles@scripps.edu; mgfinn@scripps.edu; marim@scripps.edu

The fullerene class of carbon allotropes shows promise as functional components in several emerging technologies. Properties such as high electron affinity and charge transport capabilities have made derivatives of C_{60} ("Buckyball") and carbon nanotubes particularly attractive for next-generation photovoltaic and electrical energy storage devices.[1] More recently, there has been increased interest in studying fullerenes for use in biomedicine. C_{60} has been used in gene-delivery vectors, HIV-1 protease inhibitors, magnetic resonance imaging agents, and drug delivery.[2] Because of its exceptional radical-scavenging properties, C_{60} is a promising candidate for photosensitizers in cancer therapy and the treatment of inflammatory diseases.[3]

A major drawback of C_{60} for biological applications is its insolubility in water, and numerous modifications have been made to increase its aqueous biocompatibility.[4] We describe the alternative approach of covalently attaching C_{60} derivatives to larger biological structures, in this case viral nanoparticles (VNPs). VNPs are naturally occurring self-assembling protein structures with potential applications ranging from materials to biomedicine.[5] Here we employed *Cowpea mosaic virus* (CPMV) and the capsid of bacteriophage Qβ (Figure 1A), both of which are 30 nm in size and have icosahedral symmetry. Qβ is formed from 180 copies of a single coat-protein subunit, while CPMV is composed of 60 copies of two different coat proteins, designated the large (L) and small (S) subunits. The capsid of each VNP offers multivalent attachment sites at solvent-exposed amino acids, on which diverse molecules such as redox-active moieties, imaging agents, and targeting ligands have previously been displayed.[5] The generation of aggregates of single-walled carbon nanotubes and Flock House virus has been reported.[6]

We envisioned that VNPs could serve both as hydrophilic "chaperones" for C_{60} to make the fullerene water-soluble and as platforms for the organized assembly of multiple C_{60} units in combination with other functional molecules. The specific, localized binding of C_{60} to VNP scaffolds could resolve problems of aggregation and cluster formation common to unbound fullerene derivatives. The goal of this study was to determine whether the advantages of fullerenes and VNPs could be combined by covalently attaching C_{60} derivatives to CPMV and Qβ. To test the potential of the hybrid nanomaterials as candidates for biomedical applications such as photodynamic tumor therapy, the cellular uptake of VNP$-C_{60}$ complexes in a human cancer cell line was studied.

The VNPs were decorated with C_{60} in two ways. First, the well-characterized fullerene derivative [6,6]-phenyl-C_{61}-butyric acid (PCBA) was activated by carbodiimide$-N$-hydroxysuccinimide chemistry and coupled to solvent-exposed Lys residues on CPMV and Qβ (see Figure 1B and the Supporting Information). Second, we employed the copper-catalyzed azide$-$alkyne cycloaddition (CuAAC) click reaction,[7] which has found wide application because of its high rate and specificity. CuAAC protocols for the attachment of functional molecules to VNPs with high loadings have been developed and improved in the past several years.[8] In the present case, a propargyl-O-PEG-C_{60} derivative was synthesized and conjugated to azide-modified Qβ particles using an optimized procedure[8a] (see Figure 1C and the Supporting Information), resulting in significantly higher loading than the attachment of PCBA using activated ester chemistry. In both cases, the existence of only a single linker group on each C_{60} derivative prevented covalent aggregation of the nanoparticles. The resulting hybrid complexes (VNP$-C_{60}$ and VNP$-$PEG-C_{60}) were soluble and stable in aqueous buffer solutions for at least several months.

VNP$-C_{60}$ and VNP$-$PEG-C_{60} samples were characterized by a combination of techniques. Size-exclusion chromatography (SEC; Figure 1D,E), transmission electron microscopy (TEM; Figure 1M,N), scanning transmission electron microscopy (STEM; Figure 1O), and native gel electrophoresis (see the Supporting Information) of VNP$-C_{60}$ particles confirmed their intact nature with no detectable decomposition. The covalent attachment of C_{60} was verified in both cases by Western blotting using an anti-C_{60} antibody (Figure 1H,I) and in the case of Qβ also by STEM (Figure 1O). Dynamic light scattering (DLS, Figure 1J) showed no significant changes in the apparent size of CPMV and Qβ upon attachment of C_{60}, consistent with low coverage (see below). SEC of Qβ and Q$\beta-C_{60}$ showed no change in retention time, whereas CPMV exhibited a change in retention time upon fullerene attachment (23.9 to 26.0 min). These differing SEC comparisons may reflect differing chemical interactions with the chromatography stationary phase that complicate the correlation between retention time and size. C_{60} is perhaps unusual in this respect, since it is roughly spherical and hydrophobic. Interestingly, C_{60} moieties were found attached only to the S protein of CPMV (Figure 1I), presumably at the highly reactive K38 residue.[9]

Similarly, the click reaction to prepare Q$\beta-$PEG-C_{60} gave a mixture of intact particles (peak b in Figure 1F) plus aggregated material (peak a) and broken particles (peak c). No interaction was observed between Qβ-azide and propargyl-O-PEG-C_{60} in the absence of Cu^{I}, supporting the covalent nature of the derivatization. Intact Q$\beta-$PEG-C_{60} particles were purified by SEC and reanalyzed (Figure 1G), showing a shift to shorter retention time relative to the underivatized particle (28.9 to 28.1 min), consistent with an

† Department of Cell Biology and Center for Integrative Molecular Biosciences, The Scripps Research Institute.
‡ Department of Chemistry and The Skaggs Institute for Chemical Biology, The Scripps Research Institute.
§ Department of Electronic and Nanostructured Materials, Sandia National Laboratory.
|| Department of Materials Characterization, Sandia National Laboratory.

10.1021/ja902293w CCC: $40.75

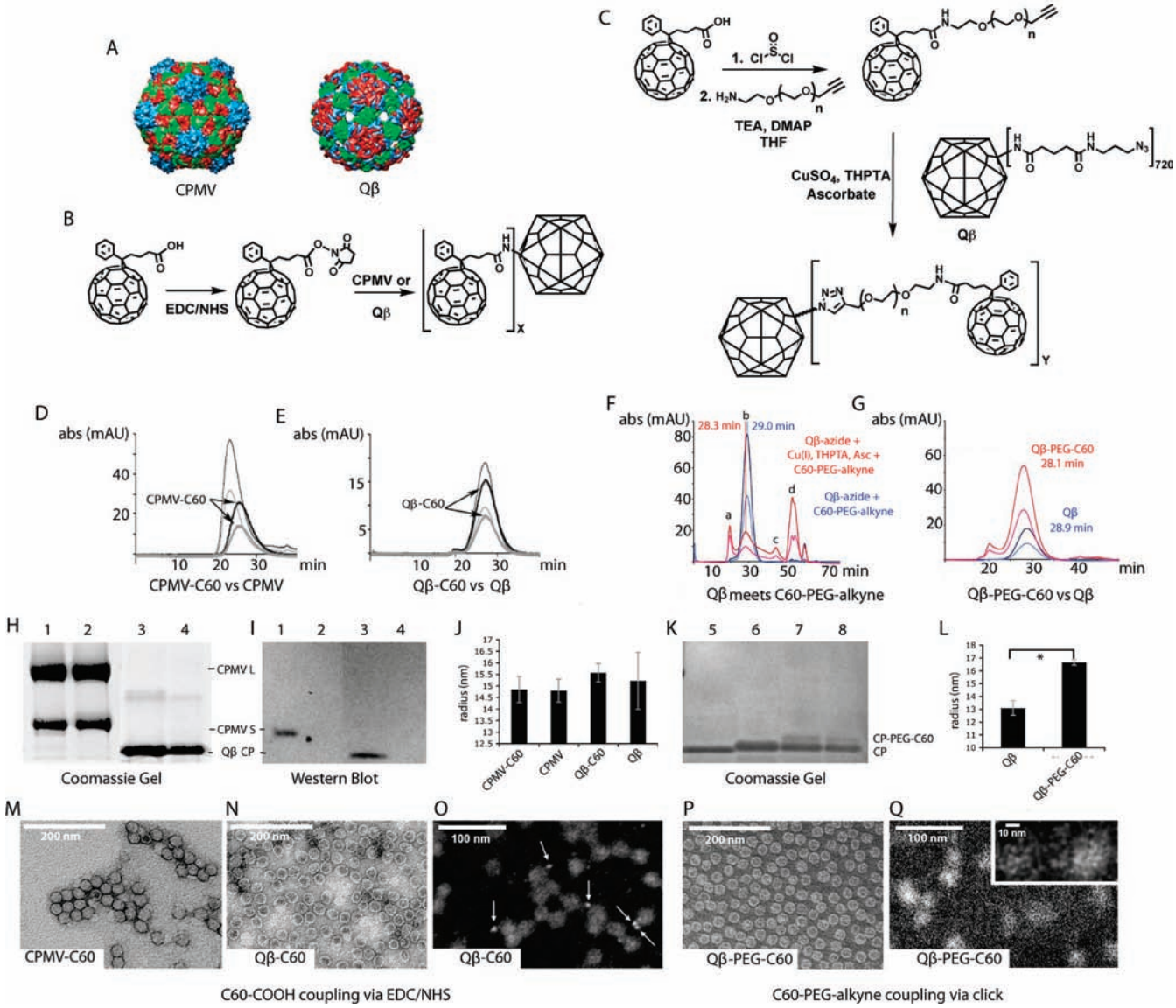

Figure 1. (A) Structure of CPMV and Qβ (reproduced from VIPERdb). (B) Derivatization of CPMV and Qβ with PCBA. (C) Derivatization of Qβ with propargyl-O-PEG-C_{60}; THPTA = tris(3-hydroxypropyl-4-triazolylmethyl)amine as an accelerating Cu-binding ligand; average $n = 20$. (D, E) SEC using a Superose 6 column (black line = absorbance at 260 nm, gray line = absorbance at 280 nm). (F) SEC of Qβ mixed with propargyl-O-PEG-C_{60} (dark blue line = 260 nm, light blue line = 280 nm) vs Qβ reacted with propargyl-O-PEG-C_{60} in the presence of $CuSO_4$, THPTA, and sodium ascorbate (red line = 260 nm, pink line = 280 nm). Peaks: a (19.6 min), VNP aggregates; b (28.3 and 29.0 min), intact Qβ−PEG-C_{60} and Qβ, respectively; c (44.9 min), broken VNPs; d (53 min), click reaction reagents (ascorbate, ligand). (G) SEC of Qβ−PEG-C_{60} after purification (red line = 260 nm, pink line = 280 nm) vs Qβ (dark-blue line = 260 nm, light-blue line = 280 nm). (H, I) Coomasie gel showing coat proteins and Western blot using anti-C_{60} specific antibodies: (1) CPMV−C_{60}; (2) CPMV; (3) Qβ−C_{60}; (4) Qβ. (J) Hydrodynamic radius as determined by DLS. (K) Coomassie gel showing the coat proteins: (5) Qβ; (6) Qβ-azide; (7) Qβ−PEG-C_{60} [aggregate, peak a of panel (F)]; (8) Qβ−PEG-C_{60} [intact VNPs, panel (G)]. (L) Hydrodynamic radius determined by DLS (* indicates significant differences with $p < 0.05$). (M, N) TEM images of uranyl acetate-stained VNP−C_{60} conjugates. (O) STEM image of OsO_4-stained Qβ−C_{60} conjugates. Arrows indicate heavily stained C_{60} nanoparticles bound around the equators of Qβ particles. (P) TEM image of uranyl acetate-stained Qβ−PEG-C_{60} conjugates. (Q) STEM image of OsO_4-stained Qβ−PEG-C_{60} conjugates. The inset reveals higher loading of VNPs with C_{60} nanoparticles, indicated by dots of bright contrast.

increase in size upon C_{60} attachment. TEM (Figure 1P), STEM (Figure 1Q), and native gels (see the Supporting Information) further confirmed the structural integrity of the Qβ−PEG-C_{60} conjugate. The hydrodynamic radius of the particle was found by DLS to increase from 13.1 nm for unmodified Qβ to 16.7 nm for Qβ−PEG-C_{60}, in good agreement with the expected dimensions of the attached species (1 nm diameter for C_{60} plus the ~2.3 nm length of the PEG-1000 chain; see the Supporting Information).

Covalent attachment of PEG-C_{60} to Qβ was further verified by the appearance of two distinct bands on denaturing gel electrophoresis, corresponding to nonlabeled and PEG-C_{60}-conjugated coat proteins (Figure 1K). Western blotting was attempted but was not successful, perhaps because of blocking of the antibody−fullerene interaction by the PEG chains (not shown).

A combination of techniques was used to quantify the degree of C_{60} loading. STEM (Figure 1O) and UV−vis absorbance spectroscopy (332 nm; see the Supporting Information) indicated sparse decoration of Qβ (~3 C_{60} molecules per particle) with PCBA using carbodiimide chemistry. This modest loading level derives from the relative aqueous insolubility of PCBA and the modest rates of amine−NHS ester reactions and is presumably similar for the analogous CPMV reactions.

In contrast, Qβ−PEG-C_{60} showed a much higher level of coverage. Individual C_{60} particles were easily visualized in large

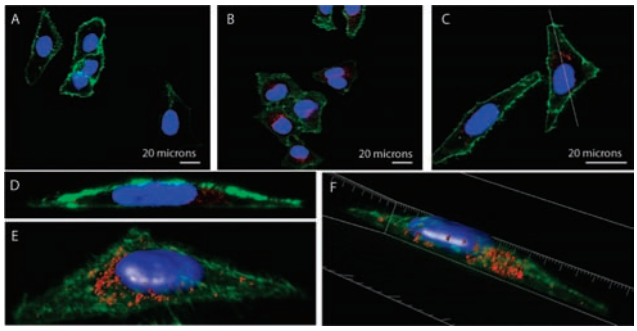

Figure 2. Confocal microscopy. (A) HeLa cells only. (B−F) Cells treated with Qβ−PEG-C_{60}−A568 particles. Color key: blue, nuclei (DAPI); red, Qβ−PEG-C_{60}−A568; green, A488-labeled wheat germ agglutinin. (D) *Z*-section image (1.2 μm deep) recorded along the line shown in (C); step size 0.3 μm. (E, F) Same cell as shown in (D), image reconstructions using Imaris software.

numbers around each VLP as dots of bright contrast in STEM images after OsO_4 staining (Figure 1Q). UV−vis spectroscopy (332 nm; see the Supporting Information) indicated a loading of 45−50 C_{60} molecules per Qβ particle. Quantitative comparison of the intensities of the derivatized and unlabeled protein bands in denaturing protein gels after Coomassie staining (Figure 1K) gave rise to a similar estimate of 30−40 C_{60} molecules per Qβ−PEG-C_{60} conjugate. The significantly greater loading is likely the result of better solubility of the PEGylated C_{60} reagent in the aqueous reaction mixture and the higher efficiency of the CuAAC reaction.

To evaluate the potential of the hybrid nanomaterials as candidates for biomedical applications, cellular uptake of dye-labeled VNP−C_{60} (see the Supporting Information) and VNP−PEG-C_{60} complexes in the HeLa human cancer cell line was studied using confocal microscopy (see Figure 2 and the Supporting Information). Qβ−PEG-C_{60} was labeled with ~60 Alexa Fluor 568 (A568) fluorophores per particle in a second CuAAC reaction (see the Supporting Information), with dye attachment being confirmed by UV−vis spectroscopy, SEC, and native and denaturing gel electrophoresis (see the Supporting Information). Cellular uptake was revealed by the acquisition of *Z*-dimensional fluorescence data (Figure 2) and found to be the same as for analogous Qβ particles bearing only the dye (data not shown), showing that internalization was not inhibited by the attached C_{60} units.

In conclusion, we have demonstrated that modified fullerene and protein nanoparticles can be covalently linked to each other with high efficiency by click chemistry, retaining the structural, spectroscopic, and biological properties of each. The hybrid VNP−C_{60}/VNP−PEG-C_{60} complexes are water-soluble and biocompatible, and the VNPs serve as scaffolds and vehicles for detectable C_{60} delivery into cells. This opens the door for the development of novel therapeutic devices with potential applications in photoactivated tumor therapy. Studies along these lines are currently under investigation in our laboratories.

Acknowledgment. We thank Dr. So-Hye Cho and Dr. Rebecca Taurog for TEM studies. This work was supported by the NIH (1K99EB009105 to N.F.S., R01CA112075 to M.M. and M.G.F., and RR021886 to M.G.F.), the American Heart Association (postdoctoral fellowship to N.F.S.), and the W.M. Keck Foundation. Work at Sandia National Laboratories was funded by the U.S. Department of Energy, Basic Energy Sciences, Materials Sciences and Engineering Division. Sandia is a multiprogram laboratory operated by Sandia Corporation, a Lockheed Martin Company, for the United States Department of Energy's National Nuclear Security Administration under Contract DE-AC04-94AL85000.

Supporting Information Available: Experimental details and supporting figures. This material is available free of charge via the Internet at http://pubs.acs.org.

References

(1) (a) Thompson, B. C.; Fréchet, J. M. J. *Angew. Chem., Int. Ed.* **2008**, *47*, 58–77. (b) Taylor, R.; Walton, D. *Nature* **1993**, *363*, 685–693.
(2) (a) Bosi, S.; Da Ros, T.; Spalluto, G.; Prato, M. *Eur. J. Med. Chem.* **2003**, *38*, 913–923. (b) Nielsen, G. D.; Roursgaard, M.; Jensen, K. A.; Poulsen, S. S.; Larsen, S. T. *Basic Clin. Pharmacol. Toxicol.* **2008**, *103*, 197–208.
(3) (a) Mroz, P.; Pawlak, A.; Satti, M.; Lee, H.; Wharton, T.; Gali, H.; Sarna, T.; Hamblin, M. R. *Free Radical Biol. Med.* **2007**, *43*, 711–719. (b) Qu, X.; Komatsu, T.; Sato, T.; Glatter, O.; Horinouchi, H.; Kobayashi, K.; Tsuchida, E. *Bioconjugate Chem.* **2008**, *19*, 1556–1560. (c) Zhao, B.; He, Y. Y.; Bilski, P. J.; Chignell, C. F. *Chem. Res. Toxicol.* **2008**, *21*, 1056–1063.
(4) (a) Andersson, T.; Westman, G.; Wennerstroem, O.; Sundhahl, M. *J. Chem. Soc., Perkin Trans.* **1994**, *2*, 1097–1101. (b) Hummelen, J.; Knight, B.; LePeq, F.; Wudl, F. *J. Org. Chem.* **1995**, *60*, 532–538. (c) Sijbesma, R.; Srdanov, G.; Wudl, F.; Castoro, J.; Wilkins, C.; Friedman, S.; DeCamp, D.; Kenyon, G. *J. Am. Chem. Soc.* **1993**, *115*, 6510–6512. (d) Sitharaman, B.; Zakharian, T.; Saraf, A.; Misra, P.; Ashcroft, J.; Pan, S.; Pham, Q.; Mikos, A.; Wilson, L.; Engler, D. *Mol. Pharmaceutics* **2008**, *5*, 567–578. (e) Vasella, A.; Uhlmann, P.; Waldruff, C.; Diederich, F.; Thilgen, C. *Angew. Chem, Int. Ed.* **1992**, *31*, 1388–1390.
(5) (a) *Viruses and Nanotechnology*; Manchester, M., Steinmetz, N. F., Eds.; Current Topics in Microbiology and Immunology, Vol. 327; Springer Verlag: Berlin, 2008. (b) Young, M.; Willits, D.; Uchida, M.; Douglas, T. *Annu. Rev. Phytopathol.* **2008**, *46*, 361–384.
(6) Portney, N. G.; Singh, K.; Chaudhary, S.; Destito, G.; Schneemann, A.; Manchester, M.; Ozkan, M. *Langmuir* **2005**, *21*, 2098–2103.
(7) (a) Kolb, H. C.; Finn, M. G.; Sharpless, K. B. *Angew. Chem., Int. Ed.* **2001**, *40*, 2004–2021. (b) Tornøe, C. W.; Christensen, C.; Meldal, M. *J. Org. Chem.* **2002**, *67*, 3057–3062. (c) Rostovtsev, V. V.; Green, L. G.; Fokin, V. V.; Sharpless, K. B. *Angew. Chem., Int. Ed.* **2002**, *41*, 2596–2599.
(8) (a) Hong, V.; Presolski, S. I.; Ma, C.; Finn, M. G. *Angew. Chem., Int. Ed.* **2009**,in press. (b) Bruckman, M. A.; Kaur, G.; Lee, L. A.; Xie, F.; Sepulveda, J.; Breitenkamp, R.; Zhang, X.; Joralemon, M.; Russell, T. P.; Emrick, T.; Wang, Q. *ChemBioChem* **2008**, *9*, 519–523. (c) Sen Gupta, S.; Kuzelka, J.; Singh, P.; Lewis, W. G.; Manchester, M.; Finn, M. G. *Bioconjugate Chem.* **2005**, *16*, 1572–1579. (d) Wang, Q.; Chan, T. R.; Hilgraf, R.; Fokin, V. V.; Sharpless, K. B.; Finn, M. G. *J. Am. Chem. Soc.* **2003**, *125*, 3192–3193.
(9) (a) Chatterji, A.; Ochoa, W.; Paine, M.; Ratna, B. R.; Johnson, J. E.; Lin, T. *Chem. Biol.* **2004**, *11*, 855–863. (b) Wang, Q.; Kaltgrad, E.; Lin, T.; Johnson, J. E.; Finn, M. G. *Chem. Biol.* **2002**, *9*, 805–811. (c) Steinmetz, N. F.; Evans, D. J.; Lomonossoff, G. P. *ChemBioChem* **2007**, *8*, 1131–1136.

JA902293W